Studying the Performance of Double Opposite Intake Canals under Different Flow Conditions

M.T. Ghonim[1], Mahmoud M Abd- Elmoneem[2], Gamal M. Abdelaal [3], and Mohamed Awad[4].
Corresponding author / mmabdelmoneem@gmail.com.
[1] Assistant professor, Water and Water Structures Engineering Department, Faculty of Engineering, Zagazig University, Zagazig, 44519 Egypt; MTGhoniem@eng.zu.edu.eg
[2] Postgraduate student, mmabdelmoneem@gmail.com.
[3] Professor of hydraulics, Water and Water Structures Engineering Department, Faculty of Engineering, Zagazig University, Zagazig, 44519 Egypt; gmal.m.mostafa60@gmail.com.
[4] Water and Water Structures Engineering Department, Faculty of Engineering, Zagazig University, Zagazig, 44519 Egypt; eng_awad2004@yahoo.com

Article History: Received: 03.01.2023 **Revised:** 20.01.2023 **Accepted:** 23.02.2023

Abstract:
This study manages the flow at the end of irrigation canals which supply the water from the agricultural open drains at high water demands for the irrigation process and controls the canal flow at low water demands. An intermediate regulator is utilized to control flow directions. Hence, the flow fluctuates and may frequently reverse Submerged hydraulic jumps have been created in a suddenly expanding stilling basin with symmetric double baffles that were investigated using both a theoretical and an experimental method in this research. The momentum and continuity formulas were used to calculate the submerged hydraulic jump depth ratio and relative energy loss theoretical equations. The flume used in the investigation was 16 m long, 65.5 cm deep, and 66 cm wide. Only one operational gate controls the flow via the regulator. The numerous changes in water directions require doubling the bed protection symmetrically. The impact of several variables, including the inlet Froude number, baffle locations, and baffle shapes, was examined. The average percentage discrepancy between theoretical and experimental findings for the depth ratio of a submerged hydraulic jump was 11.75%. From the experimental results, the square baffles (i.e., width equal to one-third of the stilling basin width at mid-distance between the double gates) provide the best jump length and energy dissipation results. Finally, these baffles increase the relative energy loss by 22% while decreasing the relative jump length by 15%.

Keywords: Submerged jump- Baffles- Regulators- Stilling basin- Energy dissipation.

Background

Potential energy changes to high kinetic energy as water flows below the gate. According to (Gehlot et al) [1], this high kinetic energy results in scour problems that might cause the hydraulic structure to collapse. The most common method for dissipating extra energy is the hydraulic jump. (Hager) [12] stated that hydraulic jumps may occur in prismatic or non-prismatic channels and can be forced or not, by safe and economical design. The position and beginning depth of the jump will determine whether it is free or submerged. (Shenglong et al.) [6] studied the features of a free hydraulic jump affected by a corrugated river bed numerically. This basin form has been found to dissipate energy 10% more than a smooth basin. The submerged jump in rectangular channels was investigated numerically by (Long et al.) [2] and (Ma et al.) [5]. The mean velocity profile and turbulence structure of the submerged jump were all predicted by the traditional k-ε turbulence model. [3] (Rao et al.) studied the characteristics of the submerged jump. For increasing submergence ratios, the energy loss in the submerged jump is less than that in the comparable free jump. (Ohtsu et al) [7] investi-

gated the change from rapid to stable flow for a submerged jump below an expanding outlet. They studied the hydraulic conditions needed for the generation of a symmetric submerged jump, and an equation for the transition between symmetric and asymmetric flows was produced. (Lopardo et al) [8] investigated the pressure variation in the SHJ basin. The experimental study allows for the computation of the coefficient of pressure amplitude of fluctuation (C'p) value for various Fn_1 and S values. The effect of a negative step and an end sill in a radial stilling basin was examined by (Negm, et al.) [9]. It is found that the end sill in a radial basin supported by a negative step reduces both depth and length ratios a little while having a slightly rising influence on the energy loss ratio. Submerged jump downstream barrage experiments were done both with and without a deflector by (Abdel-Aal [10]. It is discovered that, for various scenarios of the regulator vent operating systems, utilizing the current deflector decreases the value of the relative depth of SHJ by 8%, decreases the value of the relative jump length by 11%, and increases $\Delta E/E_1$ by 8%. (Hana, et al.) [11] studied the hydraulic jump's characteristics upstream of the sluice gate. It was discovered that the Webr number increases and Fn1 decreases when gate opening increases. Additionally, when Fn_1 rises and the Weber number decreases, there is an increase in energy loss. (Jesudhas, et al.) [13] studied a submerged jump's shear flow. The examination of the instantaneous flow characteristics reveals periodic vortex shedding to be present. A brief history of the hydraulic jump and its experimental and numerical studies were illustrated by (De Padova et al.) [29].

The stilling basin is supported by intermediate baffles to localize the hydraulic jump and dissipate more energy.

Factors such as baffle shapes and baffle locations. Many studies dealing with the effect of baffles on jump characteristics are discussed in (Rajaratnam et al.) [14], (Habibzadeh et al.) [16], (Moussa et al.) [20], and (Negm et al) [25]. The impact of the vertical baffle on the hydraulic jump and various types of jumps due to the baffle could be reviewed by (Hager et al.) [15]. (Habibzadeh et al.) [16] discovered that the efficiency of energy dissipation of submerged jumps utilizing baffles is initially larger compared to the efficiency of free jumps, but decreases as the tailwater level increases. The way the baffle blocks performed in SHJ was investigated by (Habibzadeh, et al.) [17]. The flow pattern was revealed to be either the reattaching all jet pattern, which occurs as submergence increases, or the deflecting surfaces jet pattern, which happens as submergence decreases. It was discovered that the deflected surface jet regime dissipated energy more effectively. (Y. Dilrooban) [18] examines a roughness element model in which the submergence ratio, Fn_1, roughness height, and roughness density all impact the features of SHJ. (Velioglu et al) [19] to shorten the basin's length and localize the jump location, a new structure made up of rectangular bars was examined. This model produced positive analytical and experimental results. (Moussa et al.) [20] discovered that the presence of a sill decreases the scour depth, shortens the submerged jump, and increases energy dissipation. (Al-Mansori et al) [21] examined the impact of the seven-block design on the dimensions of the stilling basin. It was discovered that the new blocks disperse energy 9.31% more than the slandered concrete baffle. Suzan et al [32] demonstrated that a screen length ratio of 0.25 was the optimal location for the screen in the contracted area. The depth and length ratio of hydraulic jump decreased by 35 percent and 40 percent, respectively, for Fn_1=4.50 and S=2.50, however, $\Delta E/E_1$ increased by 30 percent. ((Negm et al) [33] the two irregularly distributed side sills are superior to the two symmetrically distributed side sills at 0.35 numerous times the length of the basin at 0.25 and 0.50, respectively. At 0.5 times the basin length, these two symmetric sills outperform one asymmetric side sill. (Negm et al) [36] The ideal position of the curved deflector for lowering the scour dimensions for a symmetric pattern and reducing velocity vectors was discovered to be 0.06L from the rapid expansion. At this point, the relative velocity values close to the bed at the stilling basin's end are minimal,

resulting in minimum values for the relative maximum scour depth. (Herbrand et al.) [22] state that the only option for ensuring the necessary energy dissipation is lateral expansion when the tailwater level is insufficient to provide a conventional jump with the assistance of appurtenances and if excavating the basin floor is not possible due to economic considerations. (Rajaratnam et al.) [14] carried out the first investigations on abruptly expanding channels. The hydraulic jump in the non-prismatic stilling basin was investigated by (Hager et al.) [22], (Smith et al.) [23], and (Bremen et al.) [24]. (Negm, et al) [25] investigated the impact of baffle configuration on the scour depth of a rapidly enlarged stilling basin. (Daneshfaraz et al.) [26] The influence of expansion and contraction on hydraulic jump characteristics, instantaneous vertical velocities, and energy dissipation was investigated. (LUO et al.) [27] The effect of suddenly enlarged channels on the dispersion of energy in the presence of a hydraulic jump was investigated using an experimental and analytical statistical solution that yielded positive findings. (Sharoonizadeh et al.) [30] The impact of submerged counterflow jets in a suddenly enlarged stilling basin on the spatial hydraulic jump was investigated. It was found that the water jets force the jump and control the flow uniformity. (Daneshfaraz et al) [31] The influence of bat-shaped parts on a sudden expansion canal was examined. The sequent depth and S-jump length in an uneven bed decreased by 22% and 9–13%, respectively, as compared to a smooth bed. (Hasani et al) [32] the effect of the rough base on S-jump pressure changes in a rapidly enlarged stilling basin was examined. It was discovered that the creation of lateral vortices causes a rise in energy loss and a reduction in the severity of variations in pressure.

The above review demonstrates that an analysis of the substantial publication on the issue of reverse flow via an intermediate regulator indicates that there is no research published. As a result, the current work attempts to concentrate on the phenomena depicted in Fig (2).

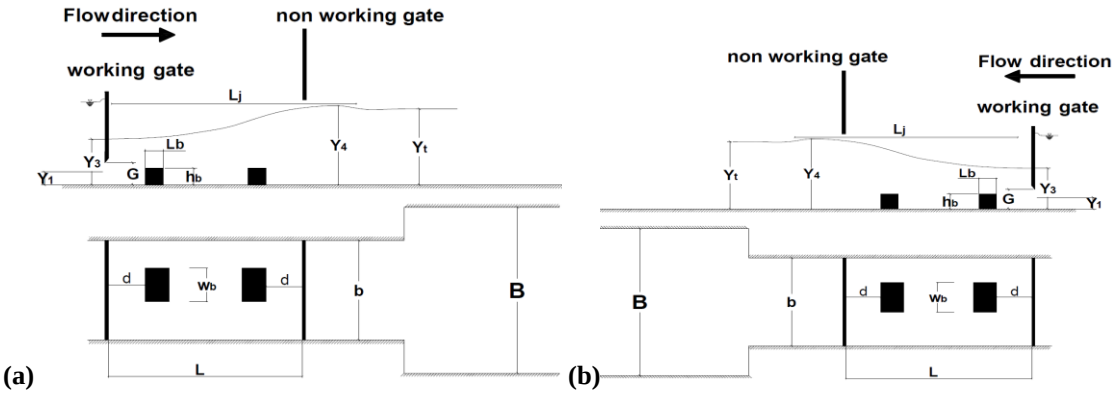

Fig 1. a,b Sketch of the experimental model, regular flow and reverse flow directions.

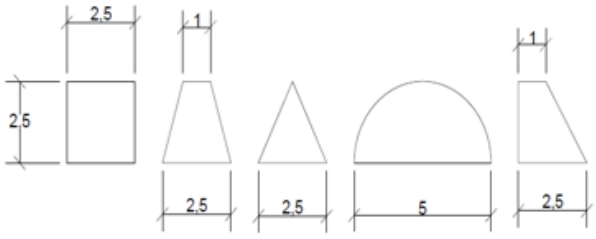

Fig 2. Different tested baffle shapes

1. Methods

A 16 m long, 65.5 cm deep, and 66cm wide recirculating flume was used for 80 laboratory experiments. The model was constructed out of clear Perspex to allow for visual inspection. The contracted

part is 48 cm wide and 160 cm long. The stilling basin abruptly expands to a width of 66cm. The model's bed is stiff. The opposing gates are 80cm apart. Each intake gate has a rapid expansion of 40cm. When the flow reverses, the basin operates with a single gate, and the non-working gate does not affect the flow conditions. Two rows of lateral central baffles with a height of 2.5cm and a width of 16cm were fastened to the basin bed at (20,30,40) cm from each intake gate, as illustrated in Fig (3). To measure discharge, a pre-calibrated rectangular weir was employed. To determine the depth of the water, a point gauge is fitted. The length of SHJ is measured using a measuring tape attached to the flume's top. The submerged jump's length is measured downstream of the roller length when the flow depth is nearly constant. To manage the submergence ratio (S), a tailgate is inserted at the channel's terminus. The depth of supercritical flow (Y_1), depth of subcritical flow (Y_t), backup water depth (Y_3), length of jump (Lj), and flow rate (Q) were all measured in a steady state. Table 1 illustrates the experimental data range.

Table.1. Experimental parameters

Symbol	Definition	Value
Q (lit/s)	Discharge	17.17-59.25
Fn_1	Inlet Froude number	1.79-8.3
S	Submergence ratio	5
E	Expansion ratio	1.4
G (cm)	Gate opening	3-4-5-6-7
d (cm)	Symmetrical baffle position from each intake gate	20-30-40
Baffle configurations	Square, semicircular, triangular, trapezoidal, and right trapezoidal as shown in Fig1.	

3.1. Results

3.1.1. Effect of baffle shape

3.1.2. The relative depth of the jump

The relationships between the relative depth of SHJ and Fn_1 are plotted for five different baffle shapes at three relative baffle positions (0.25L, 0.38L, and 0.5L), respectively, as shown in Figs. 3a, 3b, and 3c. All figures are plotted with a case of no baffle as a comparison case. These figures show a similar trend. All cases show that the relative depth of SHJ increases as Fn_1 increases at a constant S. Y_t/Y_1 decreases as the front face angle closes or is equal to 90° for a constant value of Fn_1 for all baffle positions. Y_t/Y_1 of (square, right trapezoidal, trapezoidal, triangular, and semicircle) baffles at relative position (0.5L) decreased by (27%, 23%, 22%, 16%, and 12%, respectively) compared with no baffle case at Fn_1 of 5.

(Negm et al.) [9] A smooth case curve is plotted with the presented study. Negm et al.'s submergence ratio (S = 5) results are remarkably above this study's results. This is because of the difference in the setup of the model in the two cases. Negm et al. carried out the data analysis in a gradually expanding stilling basin, while the present study was conducted in a suddenly expanding basin, which gives the lowest values of Y_t/Y_1 of SHJ. Moreover, the expansion ratio of the present study (e = 1.4) is less than the used expansion ratio (e = 1.67) of Negm.

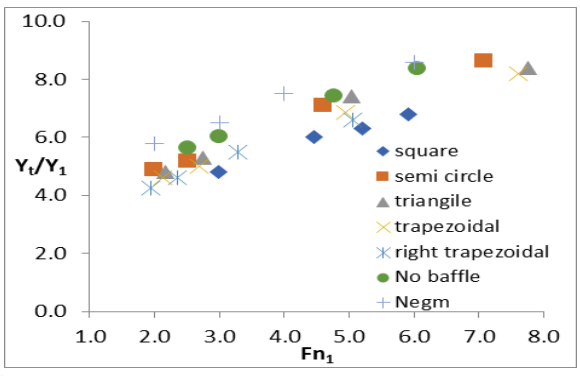

(a)

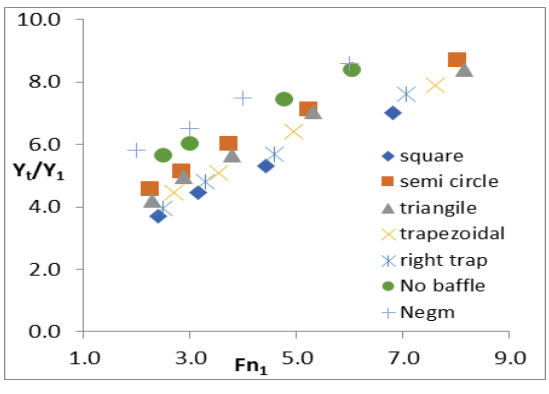

(b)

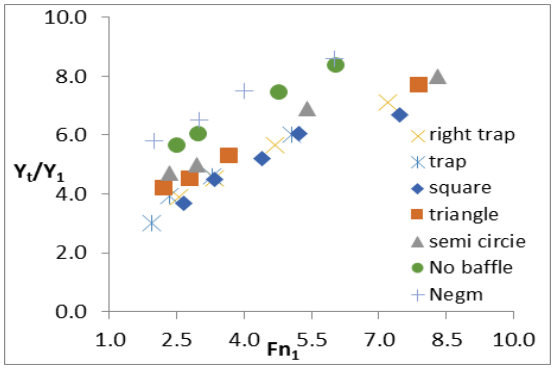

(c)

Fig 3. Relationship between Y_t/Y_1 and Fn_1 at **a** 0.25L **b** 0.38L **C** 0.5L for different baffle shapes.

3.1.3. Relative jump length:

The relation between Lj/Y_1 and Fn_1 is illustrated in Figs. 4a, 4b, and 4c. It is shown that Lj/Y_1 increases when Fn_1 increases. At Fn_1 equals 5, Lj/Y_1 of (square, right trapezoidal, trapezoidal, triangular, and semicircle) baffles decreased by (22%, 20%, 16%, 14%, and 11%), respectively, compared with no baffle case at relative position (0.5L).

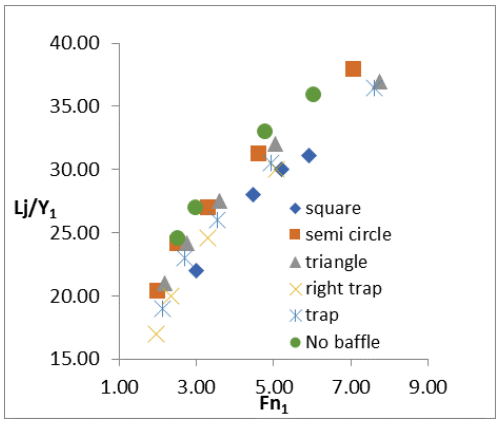

(a)

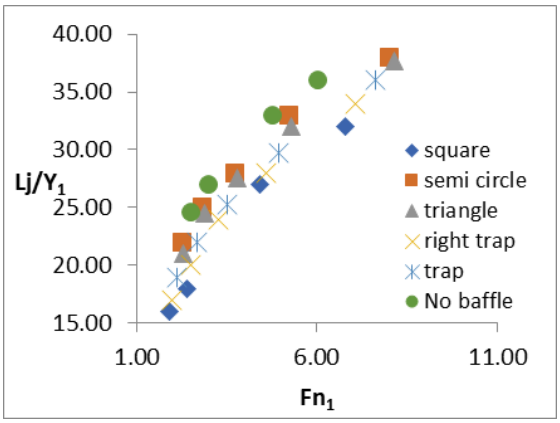

(b)

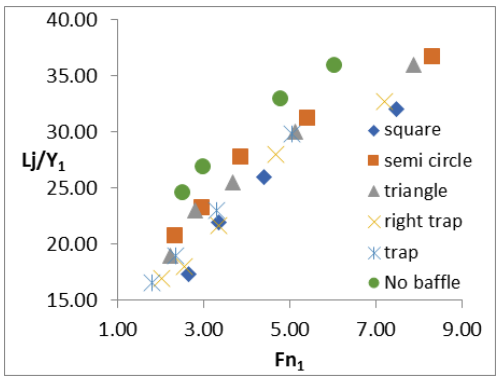

(C)

Fig 4. Relationship between Lj and Fn_1 at a 0.25L **b 038L C** 0.5L for different baffle shapes.

3.1.3. Relative energy loss:

Figs. 5a, 5b, and 5c) show the relationship between $\Delta E/E_1$ and Fn_1 for the tested baffle shapes at different locations. It is found that all cases show that $\Delta E/E_1$ increases as Fn_1 increases. At a constant Fn_1, the baffles with a vertical upstream face give the best baffle performance from $\Delta E/E_1$ point of view. While the case of no baffle shows the lowest values of $\Delta E/E_1$. $\Delta E/E_1$ of (square, right trapezoidal, trapezoidal, triangular, and semicircle) baffles at a relative position equal to 0.5L and Fn_1 of 5 increased by (15%, 10%, 9%, 7%, and 5%, respectively) compared with a no baffle case.

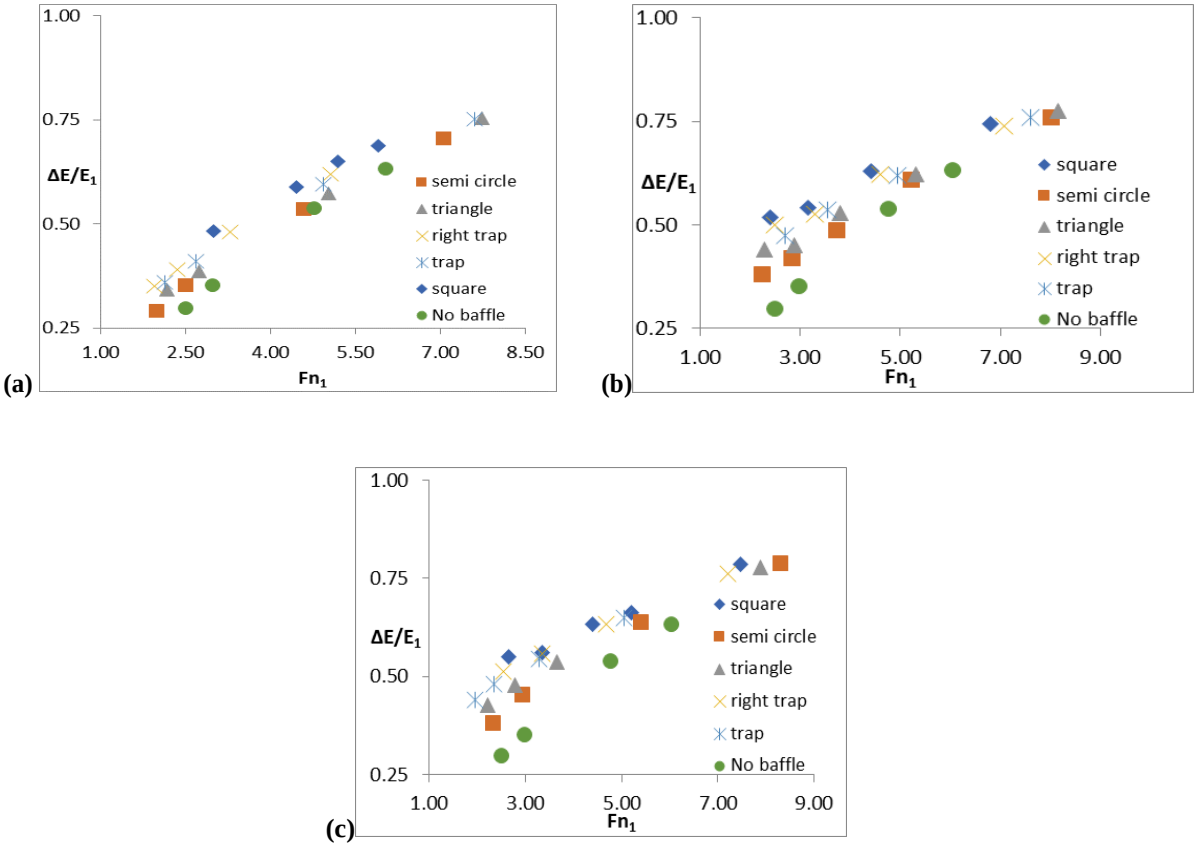

Fig 5. Relationship between $\Delta E/E_1$ and Fn_1 at **a** 0.25L, b 0.38L, and C 0.5L for different baffle shapes.

3.2. Effect of relative baffle positions

3.2.1. The relative depth of SHJ

Choosing the optimal relative placement of baffles, Y_t/Y_1 of SHJ of all the same cases of baffles (square-right-trapezoidal-trapezoidal-triangle-semicircle) is plotted against Fn_1 for different relative baffle positions (0.25L-0.38L and 0.5L) as shown in Figs. 6a, 6b, 6c, 6d, and 6e. From these figures, the relative position (0.5 L) gives the lowest values of the Y_t/Y_1 for all baffle shapes. From the experimental study, it is found that the square baffle at relative positions (0.25 L, 0.38 L, and 0.5 L) decreases the relative depth by 17%, 23%, and 27%, respectively, at a constant Fn_1 of 5.

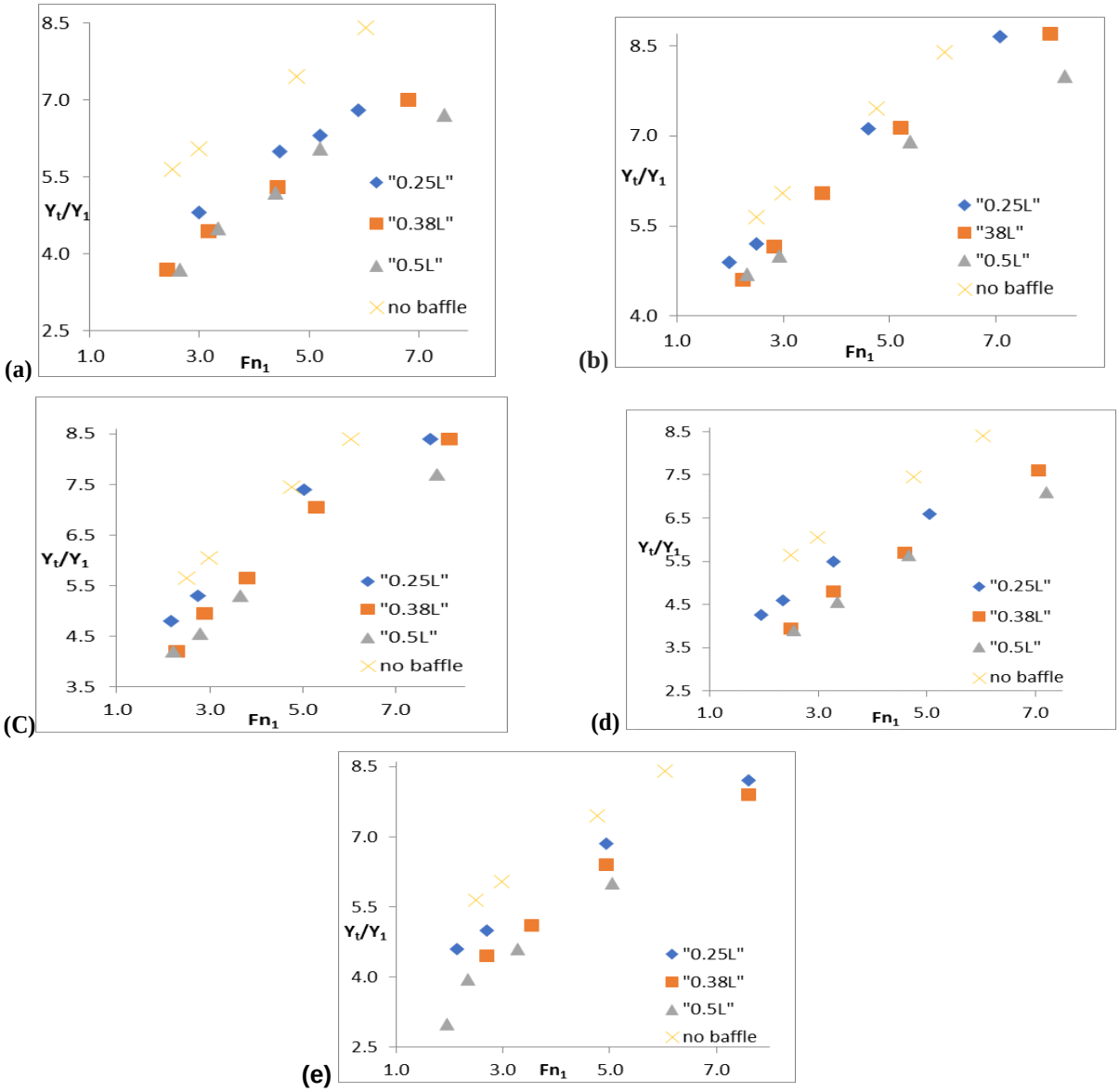

Fig 6. Relationship between Y_t/Y_1 and Fn_1 for **a** square **b** semi-circle **C** triangle **d** right trapezoidal e trapezoidal baffles at different baffle positions.

3.2.2. Relative jump length:

Figs. 7a, 7b, 7c, 7d, and 7e show the positive relationship between Lj and the Fn_1 for square, semi-circle, triangle, right trapezoidal, and trapezoidal baffles, respectively, at various baffle positions. It was found that baffles located in the middle of the basin gave the smallest values of relative length of jump for different flow conditions. From the experimental study, it is found that the square baffle at relative positions (0.25L, 0.38L, and 0.5L) decreases the relative jump length by 9%, 12%, and 15%, respectively, at a constant Fn_1 of 5.

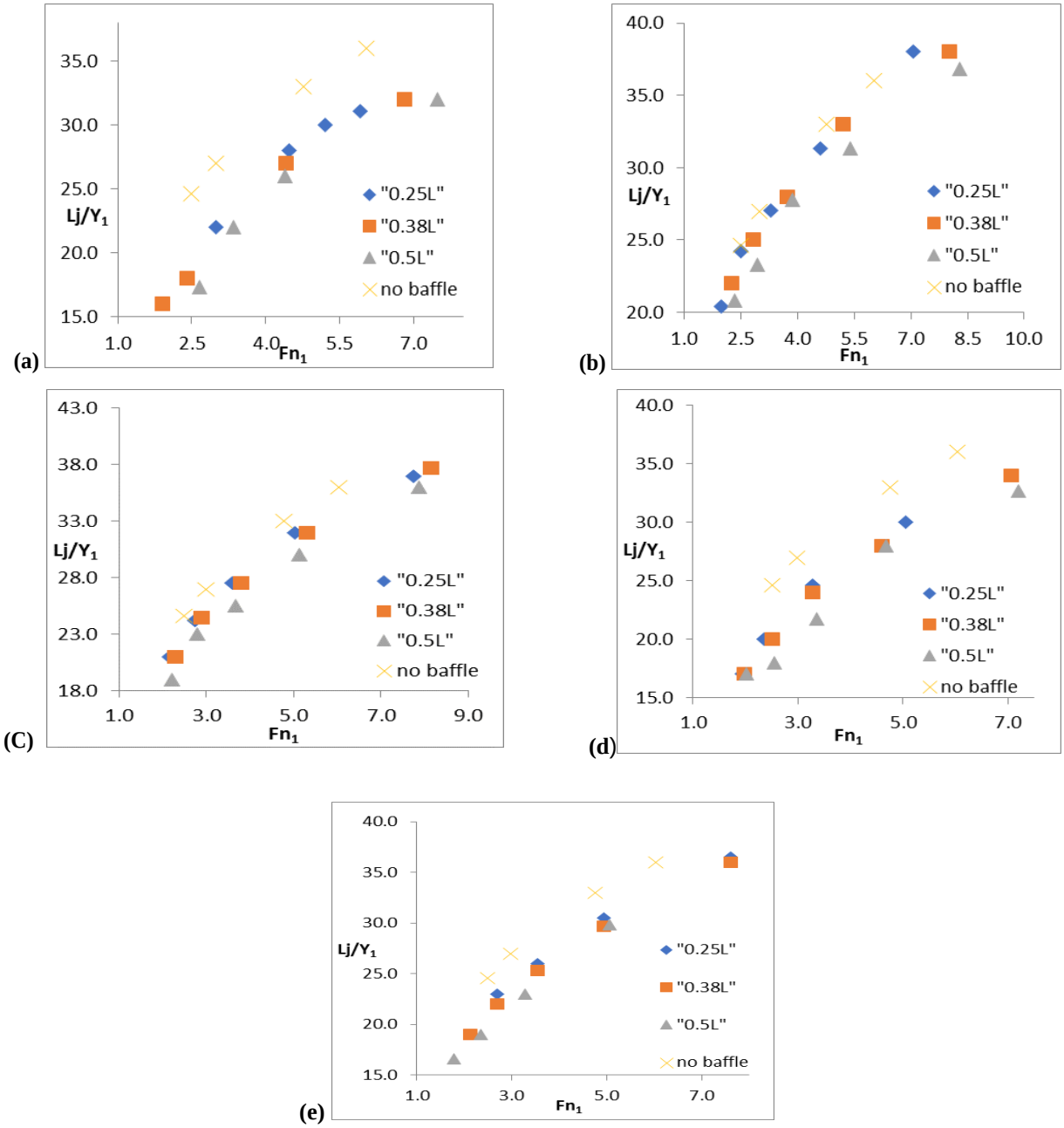

Fig 7. Relationship between Lj/Y_1 and Fn_1 for **a** square **b** semi-circle **C** triangle **d** right trapezoidal **e** trapezoidal baffles at different baffle positions.

3.2.3. Relative energy loss:

Figs. 8a, 8b, 8c, 8d, and 8e illustrate the relationship between $\Delta E/E_1$ and Fn_1 at the beginning of the sub-merged hydraulic jump. It indicates that the presence of the baffles at any location increases $\Delta E/E_1$ compared to the smooth case. From the experimental study, it is found that the square baffle at relative positions (0.25L, 0.38L, and 0.5L) increases $\Delta E/E_1$ by (13%, 19%, and 22%), respectively, at a constant Fn_1 of 5.

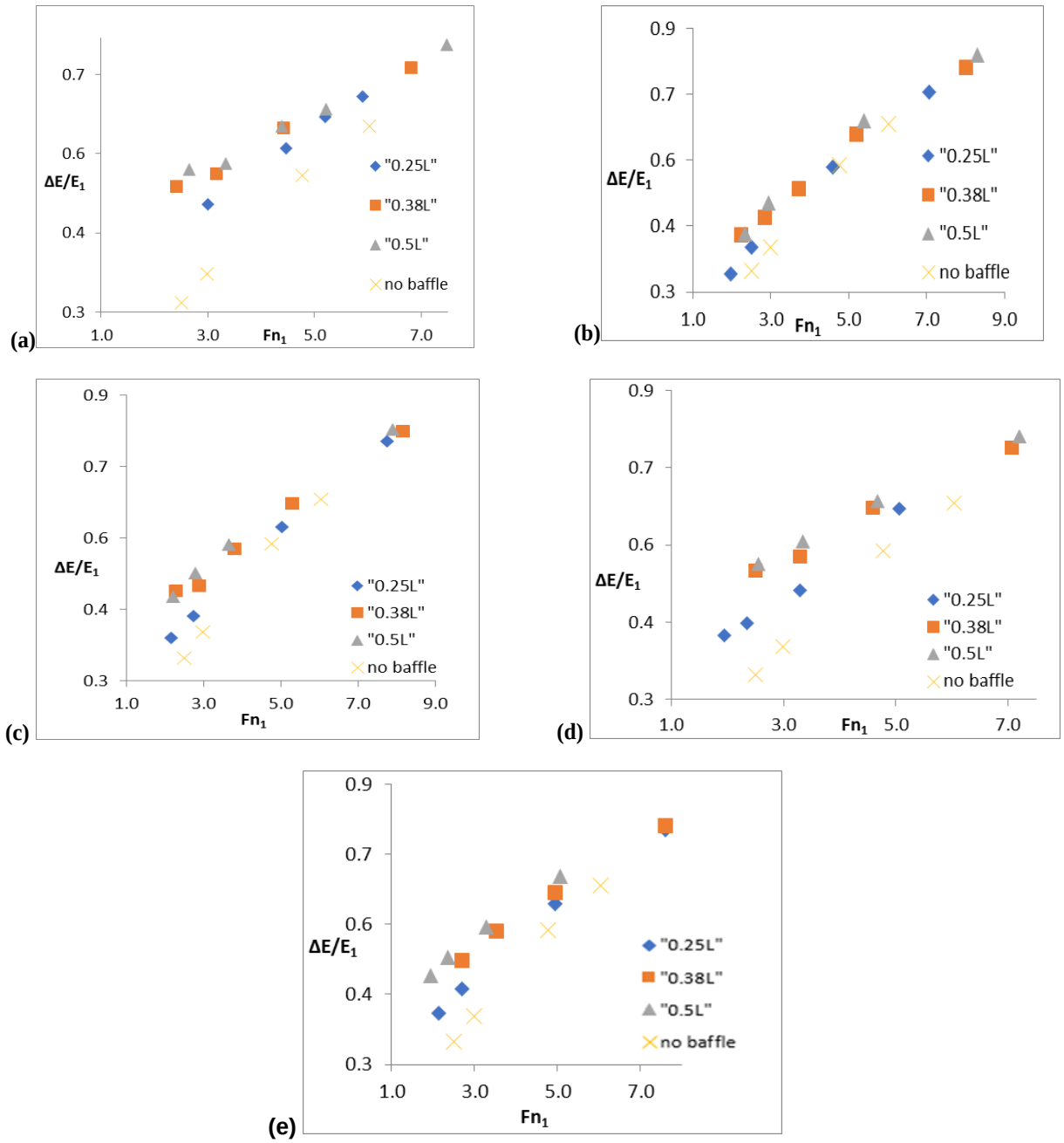

Fig 8. Relationship between $\Delta E/E_1$ and Fn_1 for **a** square **b** semi-circle **C** triangle **d** right trapezoidal **e** trapezoidal baffles at different baffle positions.

4. Discussion

4.1. Effect of baffle shape

4.1.1. Relative jump length

Lj/Y_1 increases when Fn_1 increases. This is because, at higher values of Fn_1, the jump turns out to be strong, so a larger stilling basin is required. Furthermore, at a specified Fn_1, the case of no baffle gives the longest stilling basin length. While the baffles with a vertical upstream face give the smallest values of the relative depth of SHJ due to the effect of stronger eddies and turbulence formed at the upstream sharp face of the square baffle.

4.1.2. Relative jump depth

Y_4/Y_1 increase with the increase of Fn_1 because higher Fn_1 means smaller Y_1 (at the same Q) which leads to higher (Y_t/Y_1).

4.2. Relative baffle position

4.2.1. Relative jump length

It is thought that the decrease in the subcritical depth of the jump results in the required short length to reach the jump stability. This explained why the position (0.5 L) is the best location for all baffle shapes, which gives a minimum tailwater depth and a minimum length of jump.

4.2.2. Relative jump depth

In reality, the interaction between the baffles and the incoming flow and the difference in pressure at the two sides of the baffles have a great effect on the performance of the hydraulic jump. As the flow passes downstream of the gate within the roller zone, the submerged jump's mixture of forward and reverse flow rises. This led to the negative velocity (reverse flow) increasing as the flow close to the gate, but when the flow grew farther from the gate, the positive velocity (ahead flow) decreased. Hence, the main velocity decreased at the farthest baffle position. While the difference in pressure at the two sides of the baffles increased as the baffle positions were far away from the gate. The balance of interaction behavior between the effects of pressure and impact (function of velocity and area of the baffle) of baffles achieved at the baffle location equals 0.5 L. In Bremen et al. [34], it was found that when one central lateral sill was located too close to the expansion part, the jump was over forced, so a standing wave and plunging flow were observed. The best location of the central lateral single sill within the experimental condition of this study is at a relative sill position (d/L = 0.2 to 0.3) (Negm et al.) [35]. Hasani et al. [32] examined a single perforated lateral sill with a width equal to the contracted basin width according to basin width. It was found that the best relative sill position (d/L) was 0.25. While this present study examines two adjacent central baffles with a relative width (d/L) of 0.33 in the contracted part, the best baffle location is at a relative distance of 0.5 L.

4.2.3. Relative energy loss

The impact between the inlet flow and the baffles generates eddies, water boiling, and excessive turbulence, which in turn transform the high kinetic energy to high potential energy. The mean objective of the stilling basin is to preserve the hydraulic jump with a short length and acceptable subcritical depth with high energy dissipation. These requirements are met when the baffles are located in the middle of the stilling basin.

5. Dimension analysis:

Dimensional analysis was applied to define the dimensionless parameters $\left(\frac{Y_t}{Y_1}, \frac{Lj}{Y_1}, \frac{\Delta E}{E_1}\right)$ for SHJ as shown in Fig.2. Using the principles of dimensional analysis, equation 1 may be written in the form:

$$the\ \left(\frac{Y_t}{Y_1}, \frac{Lj}{Y_1}, \frac{\Delta E}{E_1}\right) = f(d_b, Fn_1, \Pi) \quad (1)$$

6. Theoretical study:

As shown in equation (2), the 1-D momentum and continuity equations are both employed to develop a theoretical equation for determining the relative depth of SHJ generated in a suddenly expanding stilling basin with double intermediate baffles. As illustrated in Fig 9, the control volume is defined by the jump start and jump end downstream of the expansion. If the jump end is before the expanding portion, the control volume ends just before the abrupt section. The following hypotheses explain the current analysis: (a) a steady flow, and (b) an incompressible liquid. (c) the channel is horizontal with smooth edges; (d) hydrostatic pressure distribution at the start, ends, and baffles of the jump; (e) uniform velocity distribution at the control volume's beginning and ends, (f) the effects of air infiltration and turbulence are ignored, and (g) the baffles' border is smooth. The pressures at the control volume are shown in Table (2).

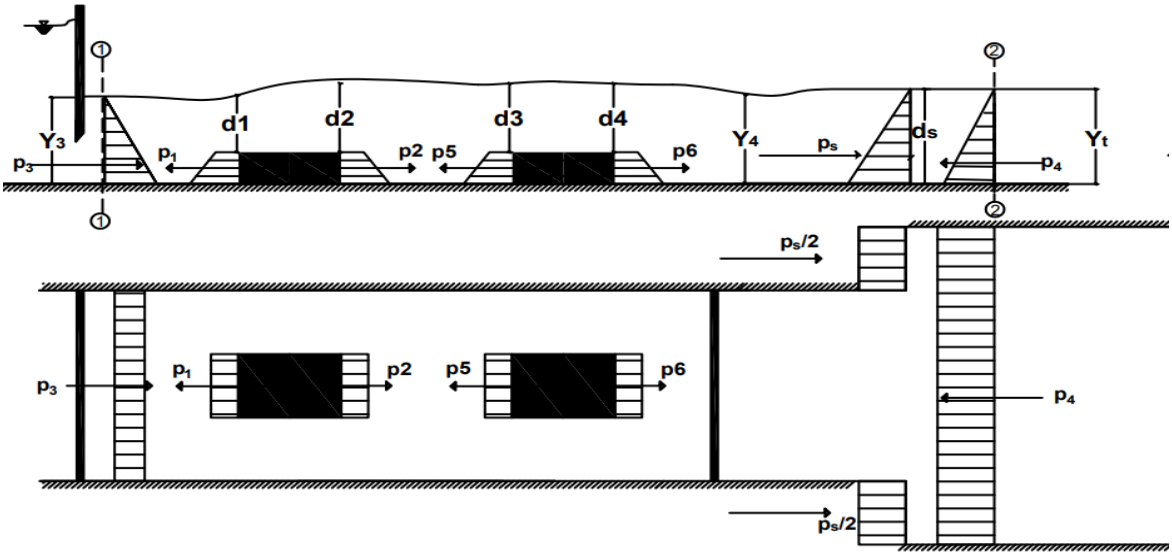

Fig 9. Definition sketch showing the momentum force.

Table.2. pressure forces at the control volume 1-2

Symbols	Definition	Control volume 1-2
P_1	Upstream hydrostatic pressure force on the first baffle	$\frac{h_b}{2}[\gamma\, d_1+ \gamma\, (d_1+h_b)]\, *W_b$
P_2	Downstream hydrostatic pressure force on the first baffle	$\frac{h_b}{2}[\gamma\, d_2+ \gamma\, (d_2+h_b)]\, *W_b$
P_3	hydrostatic pressure force at the vena contracted	$0.5\gamma * Y_3^2 *b$
P_4	hydrostatic pressure force at the end of the control volume	$0.5\ \gamma\ *Y_4^2 *B$
P_5	Upstream hydrostatic pressure force on the second baffle	$\frac{h_b}{2}[\gamma\, d_5+ \gamma\, (d_5+h_b)]\, *W_b$
P_6	Downstream hydrostatic pressure force on the second baffle	$\frac{h_b}{2}[\gamma\, d_6+ \gamma\, (d_6+h_b)]\, *W_b$
Ps	side pressure force	$0.5\ \gamma d_3^2\ *(B-b)$
P_{net}	The hydrostatic net force on the baffles	$P_2+P_6-P_1-P_5$

Based on the above, the momentum equation could be written as in equation (2) as follow:

$$P_3-P_{net}-P_s-P_4=\frac{\gamma}{g}Q(V_2-V_1) \qquad (2)$$

By substituting in eq (2):

$$0.5\ \gamma * Y_3^2 *b - \frac{h_b}{2}[\ \gamma\, d_1+ \gamma\, (d_1+h)]\, *W_b + \frac{h_b}{2}[\ \gamma\, d_2+ \gamma\, (d_2+h)]*W_b - \gamma\, d_3^2\, *(B-b) - 0.5\ \gamma\, *Y_4^2 *B = \frac{\gamma}{g}Q\,[\frac{1}{(Y4-B)} - \frac{1}{(Y1-b)}]$$

(3)

Dividing eq (3) by $(2\gamma\, y_1^2/\, b)$ and simplify to obtain**:**

$$S=\sqrt{2W_{bD}\,h_{bD}\,\Sigma d_{netD}+(e-1)d_{sD}^2+Y_D^2 e+2Fn_1^2\left(\frac{1}{eY_o}-1\right)} \quad (4)$$

In which, $e=\frac{b}{B}$, $Y_o=\frac{Y_4}{Y_1}$, $h_{bD}=\frac{h_b}{b}$, $d_{sD}=\frac{d_s}{Y_1}$, $W_{bD}=\frac{W_b}{Y_1}$ and $\Sigma d_{netD}=\frac{[d_1-d_2]}{Y_1}$

By simplifying equation (4) to get Fn_1 eq (5)

$$Fn_1=\sqrt{\frac{0.5\left(S^2-2W_{bD}\,h_{bD}\,\Sigma d_{netD}+(e-1)d_{sD}^2-Y_D^2 e\right)}{\frac{1}{eY_o}-1}} \quad (5)$$

Once the flow is reversed due to different flow conditions, the theoretical equation will be the same.

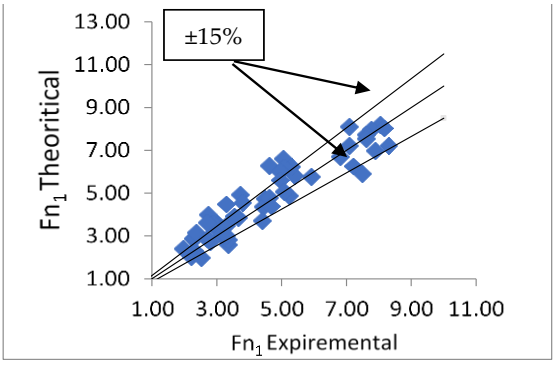

Fig 10. a Comparison of experimental and Theoretical Fn_1

The theoretical values of Fn_1 obtained by solving equation (5) for the baffles at different positions are plotted against the corresponding experimental values as illustrated in Fig (10a). Figure (10a) illustrates a little asymmetric distribution of data around the line of equality. The percentage error is ±14.87%. Almost all of the results lie between lines of (±15%) percentage errors at $Fn_1 > 3$. While at $Fn_1 < 3$ almost all the data lies above and below lines of (±15%) percentage errors. This is because the submerged jump flow reduces blending between both forward and backward flow at high submergence ratios (Ragaratnam1965) [4]. As a result, the asymmetric flow pattern downstream of the abrupt expansion recorded significant changes in side water depths. As a result, the pressure linear distribution theories are influenced by the high submergence ratio and asymmetric flow patterns. As a result, the downstream water depth at low Fn_1 recorded higher values. Besides, the baffle shape effect raises the water depth according to the impact between the inlet flow and the upstream baffles. This causes a fluctuation in water depths according to the incoming flow condition and the face angle of the baffles.

6.1. The Relative Energy loss

By applying the energy equation between sec (1) and sec (2), the energy loss is given as follows:

$$E_1=Y_3+\frac{V_1^2}{2g} \quad (6)$$

$$E_2=Y_t+\frac{V_4^2}{2g} \quad (7)$$

$$\Delta E=(E_1-E_2) \quad (8)$$

$$\Delta E/E_1=\left(Y_3+\frac{V_1^2}{2g}-Y_t-\frac{V_4^2}{2g}\right)/\left(Y_3+\frac{V_1^2}{2g}\right) \quad (9)$$

From the continuity equation:

$$V_4=\frac{V_1 Y_1 b}{Y_4 B} \quad (10)$$

Take $\frac{B}{b}=e$, $\frac{Y_4}{Y_1}=Y_D$, $V_4=\frac{V_1}{Y_D e}$, $\frac{Y_3}{Y_1}=S$

Multiply eq 9 by $\frac{Y_1}{Y_1}$ to get;

$$\frac{\Delta E}{E_1} = \frac{2S+Fn_1^2-2Y-\frac{Fn_1^2}{Y^2{}_R{}^2}}{2S+Fn_1^2} \quad (11)$$

$\Delta E/E_1$ for the baffles from the experiments and those which obtained by solving the momentum equation (1) at different locations are plotted as shown in Fig(10b).

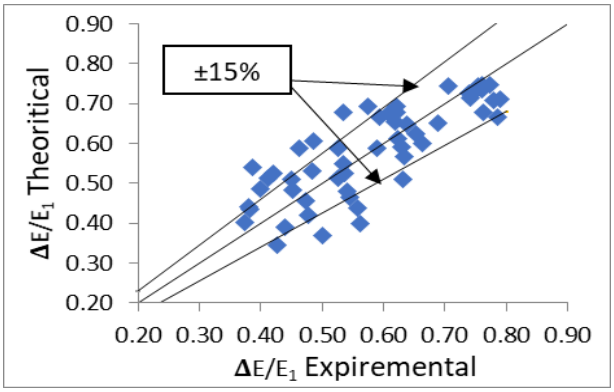

Fig 10b Experimental versus theoretical $\Delta E/E_1$.

Fig(10b) shows the relationship between the predicted $\Delta E/E_1$ computed from equation (12) and the corresponding experimental results. From this figure, there is a good distribution of data around the line of equality. The average percentage error is about ±11.75%. It is shown that about one-quarter of the collected data is above and below the line of percentage error (±15%). From Fig (4a) and Fig (4b) equations (5 and 12) may be used in the field of application to compute the theoretical Fn_1 and the corresponding $\Delta E/E_1$.

7. Conclusions

The current research could be applied to different cases around the world to manage the flow from irrigation canals to agricultural open drains and otherwise. Also, this study manages the high and low water demands by exchanging the water flow between the canals and drains. Experimental and theoretical investigations of a reverse flow in a horizontal canal with an intermediate regulator are used. Fn_1, relative baffle heights, and relative baffle widths from the gate are all investigated. Through the present study, it is concluded that:

- For all experimental models, $\Delta E/E_1$ and Lj/Y_1 and depth increase as Fn_1 increases.
- All baffles at any location within the experimental data increase $\Delta E/E_1$ and decrease Y_t/Y_1 and Lj/Y_1.
- All baffles at mid-distance between the gates give the best results which maximize the energy loss.
- The proposed theoretical equations for predicting sequent depth ratio and $\Delta E/E_1$ are well accepted with measured data.
- It was found that the square baffle gave the best performance for SHJ compared to the other tested shapes.
- Square baffles at the mid-distance of the stilling basin dissipate the extra energy by 22% and decrease both the Y_T/Y_1 and Lj/Y_1 by 27% and 13% respectively.

Abbreviations:

Y_1	Depth at Sec 1
Y_3	Backup Water Depth
Y_t	Depth at Sec 2
Lj	Length of SHJ
Ŋ	Baffle Shape coefficient
d_0	The Relative Baffle Position(d/L)
d	Baffle Distance from the Gate
L	Total Length of the Stilling Basin
Y_t/Y_1	Relative Depth of SHJ
Lj/Y_1	Relative Length of SHJ
Q	Incoming Discharge
G	Gate Opening
d_1, d_2, d_5, d_6	Water Depth above Baffles
γ	Specific Weight of the Water
ds	Water Depth at Sudden Expansion
B	Expanded Basin Width
b	Contracted Basin Width
W_b	Baffle Width
h_b	Baffle Height
h_{bo}	The relative baffle height
V_1	Average Velocity at Vena Contracta
V_4	Average Velocity at Sec 2
Fn_1	Inlet Froude Number
ΔE	Energy Loss of the Jump
E_1	Total Energy at Y_1
$\Delta E/E_1$	Relative Energy Loss
SHJ	Submerged Hydraulic Jump

8. References

1. Gehlot, Bharat Kumar, and H. L. Tiwari. "Critical review of stilling basin models for pipe outlet works." International Journal of Research in Engineering and Technology, eISSN (2014): 2319-1163.
2. Long, Dejiang, Peter M. Steffler, and Nallamuthu Rajaratnam. "A numerical study of submerged hydraulic jumps." Journal of Hydraulic Research 29.3 (1991): 293-308.
3. Rao, NS Govinda, and Nallamuthu Rajaratnam. "The submerged hydraulic jump." Journal of the Hydraulics Division 89.1 (1963): 139-162.
4. N. Rajaratnam, "submerged hydraulic jump", J. Hydraul. Div., vol.91, no. 4, pp. 71-96, 1965.
5. Ma, F., Y. Hou, and P. Prinos. "Numerical calculation of submerged hydraulic jumps." Journal of hydraulic research 39.5 (2001): 493-503.
6. Gu, Shenglong, et al. "SPH simulation of hydraulic jump on corrugated riverbeds." Applied Sciences 9.3 (2019): 436.
7. Ohtsu, Iwao, Youichi Yasuda, and Motoyasu Ishikawa. "Submerged hydraulic jumps below abrupt expansions." Journal of hydraulic engineering 125.5 (1999): 492-499.
8. Lopardo, R. A., et al. "Instantaneous pressure field on a submerged jump stilling basin." Hydraulics of dams and river structures. London: AA Balkema (2004): 133-138.
9. Negm, Abdelazim M., G. Abdel-Aal, M. Elfiky, and Y. Abdalla Mohamed. "Hydraulic Characteristics of Submerged Flow in Non-Prismatic Stilling Basins." MEJ. Mansoura Engineering Journal 28, no. 1 (2021): 19-31.
10. Abdel-Aal, G. M., et al. "Analysis and prediction of submerged hydraulic jump characteristics downstream of main barrages." Proc. of 6th Int. Conference on Environmental Hydrology and 1st Symp. on Coastal and Port Engineering. 2009
11. Hayawi, Hana A., and Ahmed Y. Mohammed. "Properties of Hydraulic Jump Down Stream Sluice Gate." Research Journal of Applied Sciences, Engineering, and Technology 3.2 (2011): 81-83.
12. Hager, W.H., 2013. Energy dissipators and hydraulic jump (Vol. 8). Springer Science & Business Media.
13. Jesudhas, V., Balachandar, R. and Bolisetti, T., 2019.Turbulent Shear Flow In Symmetric Spatial submerged hydraulic jump Journal of Hydraulic Research, 58(2), pp.335-349.
14. Rajaratnam, N. "Hydraulic jumps." Advances in hydroscience. Vol. 4. Elsevier, 1967. 197-280.
15. Hager, Willi H., and Damei Li. "Sill-controlled energy dissipator." Journal of Hydraulic Research 30.2 (1992): 165-181.
16. Habibzadeh, A., et al. "Exploratory study of submerged hydraulic jumps with blocks." Journal of Hydraulic Engineering 137.6 (2011): 706-710.
17. Habibzadeh, A., M. R. Loewen, and N. Rajaratnam. "Performance of baffle blocks in submerged hydraulic jumps." Journal of Hydraulic Engineering 138.10 (2012): 902-908.
18. Dilrooban, Y., et al. "Effect of bed roughness on submerged hydraulic jumps." (2014).
19. Velioglu, D. E. N. I. Z., NURAY DENLI Tokyay, and A. I. Dincer. "A numerical and experimental study on the characteristics of hydraulic jumps on rough beds." E-proceedings of the 36th IAHR World Congress. Vol. 28. 2015.
20. Moussa, Yasser A., M. Ali Abde-lAzim, and Yasser K. Saleh. "Performance of sills over aprons under the effect of a submerged hydraulic jump, (case study: Naga Hammadi Barrage)." Ain Shams Engineering Journal 9.4 (2018): 1365-1374.
21. Herbrand, K. "The spatial hydraulic jump." Journal of Hydraulic Research 11.3 (1973): 205-218.
22. Hager, W. H. "Hydraulic jump in non-prismatic rectangular channels." Journal of Hydraulic Research 23.1 (1985): 21-35.
23. Smith, Cliff D. "The submerged hydraulic jump in an abrupt lateral expansion." Journal of Hydraulic Research 27.2 (1989): 257-266.
24. Bremen, Roger, and Willi H. Hager. "T-jump in abruptly expanding channel." Journal of Hydraulic Research 31.1 (1993): 61-78.
25. Negm, Abdel-Azim M. "Effect of sill arrangement on maximum scour depth downstream of abruptly enlarged stilling basins." Hydraulics of Dams and River Structures: Proceedings of the International Conference, Tehran, Iran, 26-28 April 2004. CRC Press, 2004.
26. Daneshfaraz, Rasoul, et al. "Experimental investigation of hydraulic jump characteristics in contractions and expansions." Sigma Journal of Engineering and Natural Sciences 35.1 (2017): 87-98.
27. LUO, E.C.R.,2018. Analysis and Application of Hydraulic Jump with Downstream Abruptly Expanded Channel Flow.
28. Al-Mansori, Nassrin Jassim Hussien, et al. "The effects of differently shaped baffle blocks on the energy dissipation." Civil Engineering Journal 6.5 (2020): 961-973.

29. De Padova, Diana, and Michele Mossa. "Hydraulic jump: a brief history and research challenges." Water 13.13 (2021): 1733.
30. Sharoonizadeh, S., Ahadiyan, J., Scorzini, A.R., Di Bacco, M., Sajjadi, M. and Moghadam, M.F., 2021. Experimental analysis on the use of counterflow jets as a system for the stabilization of the spatial hydraulic jump. Water, 13(18), p.2572.
31. Daneshfaraz, Rasoul, et al. "Hydraulic jump in a rough sudden symmetric expansion channel." AUT Journal of Civil Engineering 5.2 (2021): 245-256.
32. Hasani, Marzieh Naem, et al. "Investigating the Pressure Fluctuations of Hydraulic Jump in an Abrupt Expanding Stilling Basin with Roughened Bed." Water 15.1 (2023): 80.
33. NEGM, Abdel-Azim M. Effect of sill arrangement on maximum scour depth downstream of abruptly enlarged stilling basins. In: Hydraulics of Dams and River Structures: Proceedings of the International Conference, Tehran, Iran, 26-28 April 2004. CRC Press, 2004. p. 181.
34. BREMEN, Roger. Expanding stilling basin. EPFL-LCH, 1990.
35. NEGM, Abdelazim M., et al. Investigating maximum scour depth downstream of abruptly enlarged stilling basins with limited lateral sills. Alexandria Engineering Journal, 2003, 42.1: 77-85.
36. NEGM, A. M., et al. The optimal position of the curved deflector to minimize scour downstream multi-vent regulators. Proc. IWTC1, 2008, 27-30.